

# The rectifying contact of hydrated multi-dimensional YSZ nanoparticles for advanced electronics

Doroshkevich A.S.<sup>1</sup>, Zakharova A.S.<sup>2,6</sup>, Oksengendler B.L.<sup>3</sup>, Lyubchik A.I.<sup>4,5</sup>, Tatarinova A.A.<sup>2,7</sup>, Kirillov A.K.<sup>2,7</sup>, Vasilenko T.A.<sup>7</sup>, Gorban O.O.<sup>1</sup>, Bodnarchuk V.I.<sup>2</sup>, Nikiforova N.N.<sup>3</sup>, Zakharova E.A.<sup>8</sup>, Balasoiu M.<sup>2,9</sup>, Mardare D.<sup>10</sup>, Mita C.<sup>11</sup>, A. Stanculescu<sup>12</sup>, Mirzayev M.N.<sup>2,13</sup>, Nabiye A.A.<sup>2,13</sup>, Popov E.<sup>2,14,15</sup>, Khiem L.H.<sup>16,17</sup>, Donkov A.A.<sup>2,18</sup>, Konstantinova T.Ye.<sup>1</sup>

<sup>1</sup> Donetsk Institute for Physics and Engineering named after O.O. Galkin, Kiev, Ukraine, e-mail: [doroh@jinr.ru](mailto:doroh@jinr.ru);

<sup>2</sup> Joint Institute for Nuclear Research, Dubna, Russia, e-mail: [doroh@jinr.ru](mailto:doroh@jinr.ru);

<sup>3</sup> Ion-plasma and laser technologies Institute after U. Arifov, Uzbekistan, Tashkent, e-mail: [oksengendlerbl@yandex.ru](mailto:oksengendlerbl@yandex.ru);

<sup>4</sup> Nanotechcenter LLC, Krzhizhanovsky str., 3, Kyiv 03680, Ukraine e-mail: [andrey.lyubchik@campus.fct.unl.pt](mailto:andrey.lyubchik@campus.fct.unl.pt);

<sup>5</sup> Research Centre in Industrial Engineering Management and Sustainability, Lusófona University, Campo Grande, 376, 1749-024 Lisbon, Portugal, e-mail: [andrey.lyubchik@campus.fct.unl.pt](mailto:andrey.lyubchik@campus.fct.unl.pt);

<sup>6</sup> Dubna State University, Dubna, Russia, 19 Universitetskaya street, Dubna, Moscow region, 141982 e-mail: [zakharova.anna.nano@gmail.com](mailto:zakharova.anna.nano@gmail.com)

<sup>7</sup> Saint-Petersburg Mining University, St.-Petersburg, Russia e-mail: [kirillov1953@inbox.ru](mailto:kirillov1953@inbox.ru).

<sup>8</sup> Institute of Oil Refining and Petrochemistry FSBEI of HE USPTU, Salavat, Russia, e-mail: [sacharova\\_08@mail.ru](mailto:sacharova_08@mail.ru)

<sup>9</sup> Horia Hulubei National Institute for R&D in Physics and Nuclear Engineering (IFIN-HH), Bucharest Romania, e-mail: [masha.balasoiu@gmail.com](mailto:masha.balasoiu@gmail.com);

<sup>10</sup> Faculty of Physics, "Alexandru Ioan Cuza" University of Iasi, Bld. Carol I, No. 11, 700506 Iasi, Romania; [dianam@uaic.ro](mailto:dianam@uaic.ro);

<sup>11</sup> Faculty of Chemistry, "Alexandru Ioan Cuza" University of Iasi, Bld. Carol I, No. 11, 700506 Iasi, Romania; [cmita@uaic.ro](mailto:cmita@uaic.ro);

<sup>12</sup> Optical Processes in Nanostructured Materials Laboratory, National Institute of Materials Physics, 405A Atomistilor Street, P.O. Box MG-7, 077125 Magurele, Romania; e-mail: [sanca@infim.ro](mailto:sanca@infim.ro);

<sup>13</sup> Institute of Radiation Problems, Azerbaijan National Academy of Sciences, Baku, AZ1143, Azerbaijan; e-mail: [matlab@jinr.ru](mailto:matlab@jinr.ru);

<sup>14</sup> Institute of Solid-State Physics, Bulgarian Academy of Sciences, Sofia, 1784, Bulgaria; e-mail: [epetropov@gmail.com](mailto:epetropov@gmail.com);

<sup>15</sup> Institute for Nuclear Research and Nuclear Energy, Bulgarian Academy of Sciences, Sofia 1784, Bulgaria;

<sup>16</sup> Graduate University of Science and Technology, Vietnam Academy of Science and Technology, 18 Hoang Quoc Viet, Cau Giay, Ha Noi, Viet Nam, e-mail: [lhkhiem@iop.vast.ac.vn](mailto:lhkhiem@iop.vast.ac.vn).

<sup>17</sup> Institute of Physics, 10 Dao Tan, Ba Dinh, Ha Noi, Viet Nam,

<sup>18</sup> G.Nadjakov Institute of Solid State Physics, Bulgarian Academy of Sciences, 1784, Sofia, Bulgaria e-mail: [aadonkov@yandex.com](mailto:aadonkov@yandex.com)

\*E-mail: [doroh@jinr.ru](mailto:doroh@jinr.ru)

## Abstract

The paper considers new effects of the nanoscale state of matter, which open up prospects for the creation of electronic devices using new physical principles.

The contact of chemically homogeneous different sizes hydrated nanoparticles of yttrium-stabilized zirconium oxide ( $\text{ZrO}_2 - x \text{ mol } \text{Y}_2\text{O}_3$ ,  $x=0, 3, 4, 8$ ; YSZ) with particle sizes of 7.5 nm and 7,5 nm; 7.5 nm and 9 nm; 7.5 nm and 11 nm; 7.5 nm and 14 nm in the form of compacts obtained using high hydrostatic pressure (HP-compacts of 300MPa) was studied at direct and alternating current. A unique size effect of the nonlinear (semiconductor) dependence of the electrical properties (in the region  $U < 2.5 \text{ V}$ ,  $I \leq 2.7 \text{ mA}$ ) of the contact of different-sized YSZ nanoparticles of the same chemical composition is revealed, which indicates the possibility of creating semiconductor structures of a new type based on chemically homogeneous nanostructured systems.

The electronic structure of the near-surface regions of nanoparticles of a special type of oxide materials and the possibility, on this basis, to obtain specifically rectifying properties of the contacts were studied theoretically.

Models of surface states of the Tamm type are constructed, but considering the Coulomb long-range action.

The discovered variance and its dependence on the curvature of the surface of nanoparticles made it possible to study the conditions for the formation of a contact potential difference in cases of nanoparticles of the same radius (synergistic effect), different radii (doped and undoped variants), as well as to discover the possibility of describing a group of powder particles from material within the Anderson model.

The established effect makes it possible to solve the problem of diffusion instability of semiconductor heterojunctions and opens up prospects for creating electronics devices with a fundamentally new level of properties for use in various fields of the national economy and breakthrough critical technologies.

## 1. Introduction

Diffusion instability of classical semiconductor structures [1], leading to inevitable failures of electronic equipment, is a serious scientific and technical problem of modern critical technologies [2].

There are a number of theoretical works that discuss possible ways to solve this problem [3, 4, 5, 6, 7], however, so far it has not been possible to find possible options for the practical implementation of devices devoid of this drawback. According to the authors of this work, the problem can be solved by using new physical principles in the creation of functional semiconductor structures, in particular, the effects of the low-dimensional state of matter [8]. The concept of the work is the replacement of semiconductor heterojunctions, in which excess charge carriers are formed by implanting a non-valent impurity with functional junctions, in which excess charge carriers are formed as a result of size effects of band structure distortion (nanoscale objects).

The nanopowder system based on  $\text{ZrO}_2$  is characterized by dimensional effects of an adsorption nature and therefore, is interesting for practical application. In particular, the previously determined effects, such as adsorption-induced electrical conductivity [9], localization and transport of charge carriers to electrodes [10, 11], accumulation of electric charge [12, 13], and the size effect of the appearance of periodic current pulsations in compacts of zirconium dioxide nanopowder during a discharge after exposure to a constant current [14] against the background of a finite electrical conductivity (ionic conductivity) of the system, indicate the presence of adsorption-induced interphase electron exchange and its electrical continuity. Therefore, it is possible to generate and remove nonequilibrium charge carriers from the functional layer, which is formed upon contact of two nanoparticles of the same chemical composition, but with different surface geometry (particle size) due to the size effect of energy band distortion. Therefore, a hydrated nanopowder system based on  $\text{ZrO}_2$  can be used to implement a new type of functional transition. Study of the electrical properties of the contact of hydrated nanopowder YSZ systems is the aim of this work.

## 2. Devices and materials

The sample is a contact of two compacts of nanopowders of the composition  $\text{ZrO}_2 - 3 \text{ mol\% Y}_2\text{O}_3$  with a particle size of 7.5 and  $x \text{ nm}$ , where  $x = 7.5 \text{ nm}$  (400);  $10 \text{ nm}$  (500);  $12 \text{ nm}$  (600);  $14 \text{ nm}$  (700) [15] in the tablet form (Fig. 1,a).

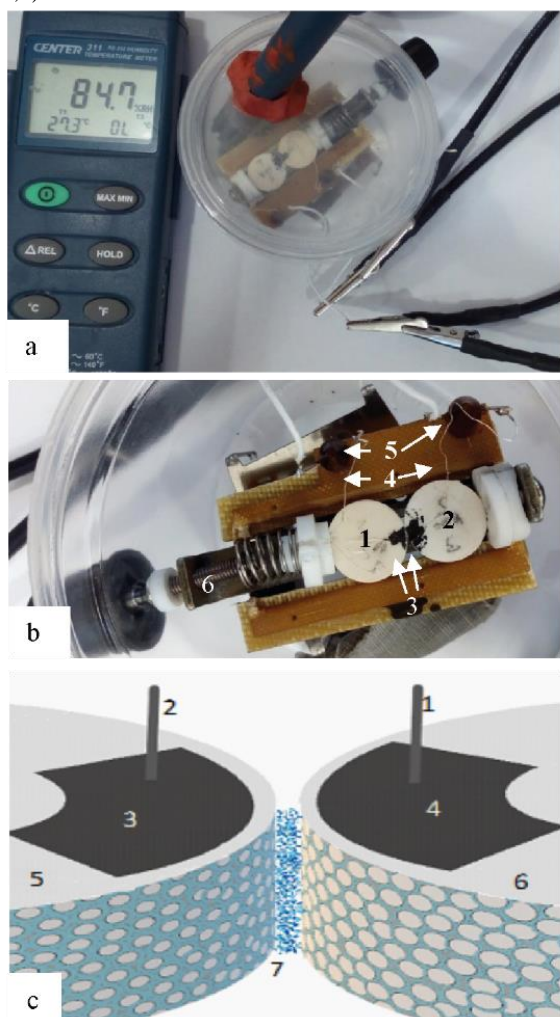


Fig. 1 External view of the sample chamber (a) and the sample holder (b), where 1, 2 - the tablets under study; 3- contact pads; 4- current collectors; 5 - fixing racks; 6 - mechanical spring-loaded clamp with adjustable force. The scheme of the experiment, where 1 - anode, 2 - cathode, 3,4 - contact pads; 5 - a tablet of a powder with a smaller particle size, 6 - a tablet of a powder with a large particle size, 7 - a hydration layer.

To obtain nanopowders, the chemical technology of co-deposition with the use of physical effects was used [16]. First, hydrated zirconium hydroxide was obtained by precipitation from chloride raw materials. After dehydration in a special microwave oven ( $T = 120 \text{ }^{\circ}\text{C}$ ,  $t = 0.4 \text{ h}$ ), the amorphous powder was subjected to crystallization annealing for 2 h at  $400 \text{ }^{\circ}\text{C}$  for the 5 (Fig. 1) and at  $500 \text{ }^{\circ}\text{C}$  for the 6 (Fig. 1) contacting object.

The compacts were obtained from powders of the composition  $\text{ZrO}_2 - 3 \text{ mol\% Y}_2\text{O}_3$  by uniaxial pressing ( $P_{\text{comp}} = 40 \text{ MPa}$ ) in the form of tablets with a diameter of 20 mm and a height of 3.2 - 3.3 mm (weighed amount  $m = 1.2 \text{ g}$ ), then compaction was made with high hydrostatic pressure (HHP, 300 MPa) in the installation type UVD-2. HHP diameter of the compacts decreased on average to 16mm, and the height - to 2mm.

The sample chamber was a closed container with a volume of 350 ml with the atmospheric humidity controlled using salts [17] (Fig. 1a).

The sample under study was a contact of two tablets of nanopowders with the composition  $\text{ZrO}_2 - 3 \text{ mol\% Y}_2\text{O}_3$  with particle sizes of 7.5 and 10 nm (Fig. 1c).

Current collectors made of tinned copper wire 0.01 mm in diameter were glued to the ends of the tablets (1, 2) near one of the edges using a conductive varnish based on nickel powder (MASTIX) specifications 2262-018-90192380-2011 (Fig. 1, b). Conductive areas (3) formed during the drying of conductive graphite varnish, to which the current

collectors (4) were glued served as electrodes. The area of the electrodes was about 3 mm<sup>2</sup>. Current collectors were fixed on special fixing racks (5). From the racks, wires were leading directly through the walls of the chamber. The positive electrode "+" was connected to compact 400, and the negative electrode "-" to compact x. The tablets were in contact with the help of a special mechanical spring-loaded clamp (6) with anadjustable force (about 10 N). The shape of the contacting surfaces of the tablets was elliptical.

The sample chamber was a closed container with a volume of 350 ml with controlled using salts KCl (60%), NaCl (76%) and NaBr (86%), atmospheric humidity.

The spatial and structural organization of the samples was investigated by transmission (TEM) and scanning (SEM) electron microscopy using JEM 200A and JSM640LV instruments.

Voltammograms (VAC) were obtained in a linear sweep mode (from - 6V to + 6V) on an R-20 device ("Elinns") in a moisture saturation mode at three points (86, 76, and 60%). The experiment was carried out in 3-fold repetition.

The positive electrode was placed on a powder tablet with smaller nanoparticle size. The sequence of measuring electrical parameters: from maximum (humidity = 86%) - to minimum (humidity = 60%). The saturation times of the samples at each humidity are at least 2 hours (until the adsorption equilibrium is established in the system: working volume - salt - sample) with an accuracy of 5%.

### 3. Results

#### 3.1. Morphology of the studied objects

TEM images of nanopowders of the composition ZrO<sub>2</sub> - 3 mol% Y<sub>2</sub>O<sub>3</sub> obtained at calcination temperatures of 400 °C and 500 °C are shown in Fig. 2. The figure shows that nanoparticles form relatively loose aggregates up to 1 µm in size in the case of a powder obtained at 400 °C, and no more than 300 nm in the case of a powder obtained at 500 °C. Therefore, the 9nm powder is better distributed over the substrate than the 7.5 nm powder. This indicates a lesser cohesion of particles in it. Tablets made of nanopowders have approximately the same density (approximately 3g / cm<sup>3</sup>) and porosity of about 50% [18].

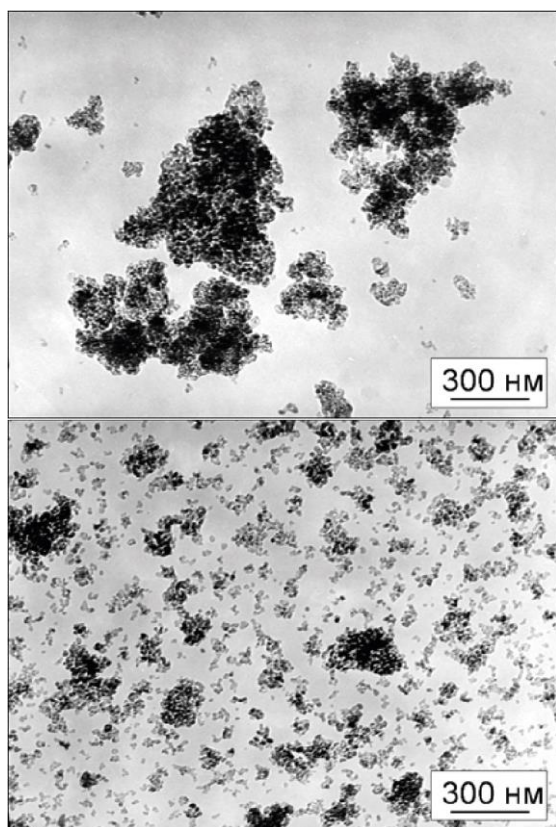


Fig. 2. TEM images of nanopowders of the composition ZrO<sub>2</sub> - 3% mol Y<sub>2</sub>O<sub>3</sub>, obtained at annealing temperatures of 400 °C (a) and 500 °C (b).

The SEM image (Fig. 3) shows the fracture morphology of the compact. A significant number of relatively large (about 1 µm) pores can be seen, obviously serving as channels for moisture penetration into the bulk of the compact material. Consequently, moisture relatively easily penetrates the bulk of the samples and the limiting time factor is its adsorption by the interface [19].

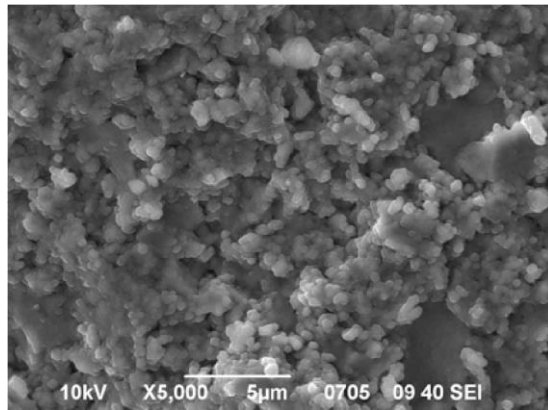


Fig. 3. A typical SEM image of a fracture in a nanopowder compact with the composition  $\text{ZrO}_2$  - 3% mol  $\text{Y}_2\text{O}_3$ . (The nanopowder was obtained at a calcination temperature of 400 °C).

To compensate for the valence-unsaturated electron orbitals of surface atoms - chemically active centers,  $\text{ZrO}_2$  nanoparticles sorb electrically neutral molecules mainly water from the gas atmosphere, [20]. When interacting with a surface, a molecules are polarized (in the case of physical contact) or exchange electrons if the interaction is chemical. Thus, as a result of the implementation of adsorption processes, the surface of nanoparticles is covered with an electrically conductive hydration shell [21,22], due to which the continuity of the electrical properties of the compact material is realized. It should be noted that the quantitative composition of the adsorption shell of nanoparticles, and as a consequence, the electrical conductivity of the nanopowder system dynamically changes with a change in atmospheric humidity.

### 3.2. Contact of different sized nanoparticles.

Figure 4 shows the current versus voltage dependences obtained at an atmospheric humidity of 85%. It can be seen that the dependence of the current on the voltage for the contact of systems with the same particle size (curve 400 - 400) on a given scale has a linear character, while a similar dependence for the contact of systems with different sizes of nanoparticles (curve 400 - 500) has a pronounced "diode" character in the voltage range from  $-5$  to  $+2$  V. The forward branch of the semiconductor junction with the used arrangement of the electrodes is in the fourth octant, the reverse branch is in the first (Fig. 4). The linear nature of the heterojunction between compacts with the same particle size (400-400) indicates a relatively low current (up to 20  $\mu\text{A}$ ) through the contact at the specified humidity. The contact of compacts of different-sized particles at the same moisture content demonstrates an order of magnitude higher (up to 250  $\mu\text{A}$ ) current.

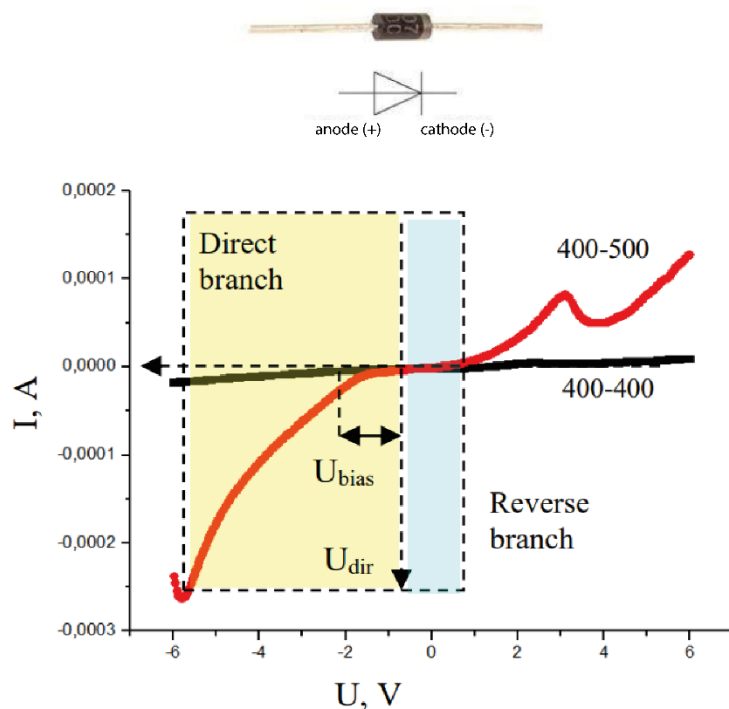


Fig.4. A V-I curves of contacts of chemically identical samples ( $\text{ZrO}_2$ -3 mol%  $\text{Y}_2\text{O}_3$ ) with identical size of particles (curve 400-400) and samples with different size of particles (curve 400-500) at humidity (85%).



The working range of the obtained heterojunction is about 5V - forward branch, 2V - reverse. After exceeding these values, the loss of its straightening properties occurs. The curve is offset from zero to negative values. It can be assumed that the presence of a bias voltage of -2V is due to the polarization of the contact or electrodes.

### 3.3. Influence of humidity and particle size difference on the electrical properties of the contact.

The thickness and conductivity of the hydration layer depend on the particle size [21] and the atmospheric humidity. The hydration shell is continuous under normal conditions for systems with a particle size of up to 9 nm (annealing temperature of 500 °C). Above 14 nm (annealing temperatures above 700 °C), the hydration shell has an “island” character [23]. Conductivity in the system occurs when the hydration shells of individual nanoparticles overlap; therefore, there is a percolation threshold for electrical properties.

In Fig. 5. V-I dependences of four contacts formed by chemically homogeneous nanostructured objects, differing in the difference in the sizes of nanoparticles after hydration in an atmosphere with different concentrations of moisture vapor, are presented on an optimized scale. At lower humidity, the system is beyond the percolation threshold in a nonconducting state [24, 25] and cannot be investigated by the measuring instruments used in this work.

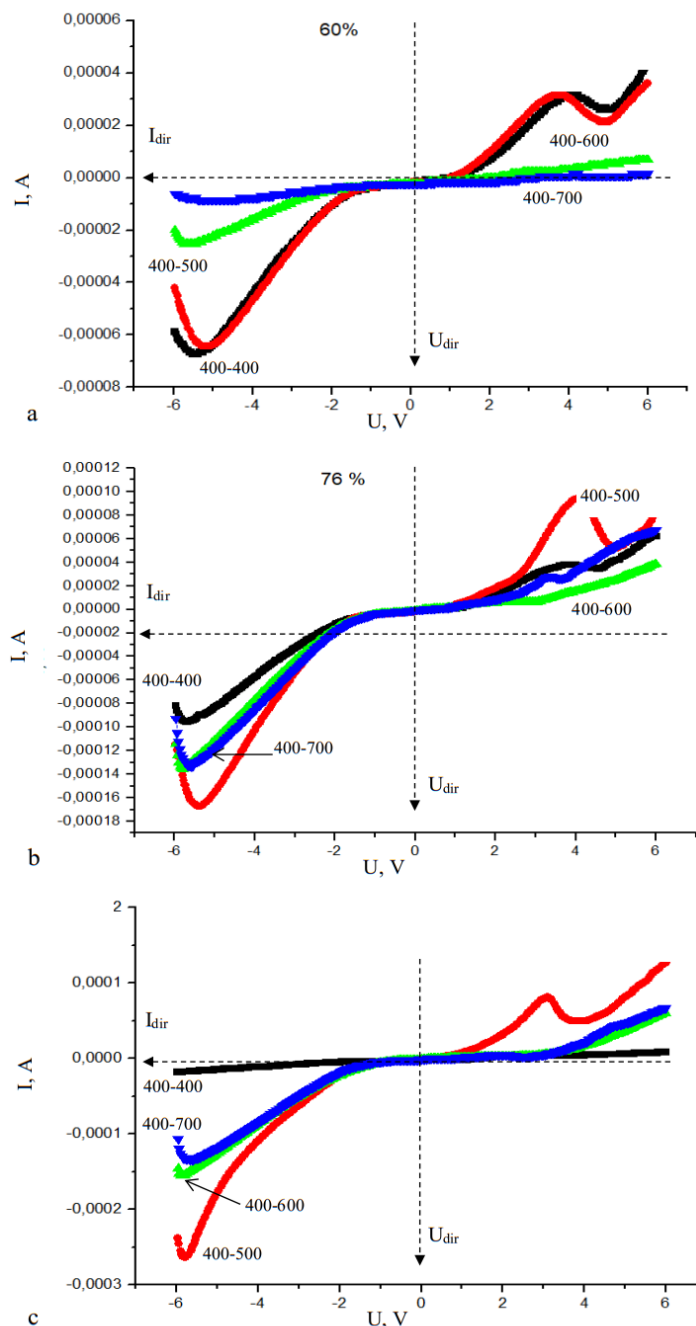


Fig.5. A V-I curves family of contacts of chemically identical samples ( $\text{ZrO}_2$ -3 mol%  $\text{Y}_2\text{O}_3$ ) with identical size of particles 7.5nm (curves 400-400) and samples with different size of particles: 7.5nm – 9nm (curves 400-500); 7.5nm – 11nm (curves 400-600); 7.5 – 14nm (curves 400-700) at humidity 60% (a), 76% (b) and 86% (c).

Fig. 5a, it can be seen that at low humidity the group of contacts 400-600 and 400-700 differs significantly like the V-I characteristic from the group of contacts 400-400 and 400-500 by extremely low operating currents. The characteristic features in the range of voltage values of - 5V and + 4V on the curves are also very weakly expressed. It can be assumed that, in contrast to mutually well-hydrated low-dimensional systems 400-400 and 400-500, systems containing larger particles (11 and 14 nm for powders obtained, respectively, at 600 °C and 700 °C) at a humidity of 60% are close to the threshold of electrical percolation. Contacts 400-600 and 400-700 have a slightly increasing linear characteristic. Systems 400-400 and 400-500 exhibit the properties of a "false" compound at 60% humidity [26], in which Ohm's law is violated due to electrophysical transient and resonance processes.

At a humidity of 76% (Fig. 5b), contacts 400 - 400 and 400 - 500 begin to change their behavior significantly: I-V contacts 400 - 400 begin to level out, and I-V contacts 400-500, on the contrary, bend and "turn" into a rectifying one. Contacts 400 - 600 and 400 - 700 have virtually indistinguishable I-V characteristics of the rectifier type. The trend persists with a further increase in atmospheric humidity (saturated vapor pressure). At 85%, their limiting characteristics differ from those for a 400-500 contact by half the limiting forward current (1.4-1.5mA and 2.7mA), and almost twice the reverse voltage, 1.8V, and 3.5V.

The peak in the + 3V region is probably due to water dissociation processes. The peak at  $U = -6 - -5.5V$  on the forward branch is probably a concentration limitation on the majority charge carriers. It can be concluded that the majority of charge carriers in this system are positively charged.

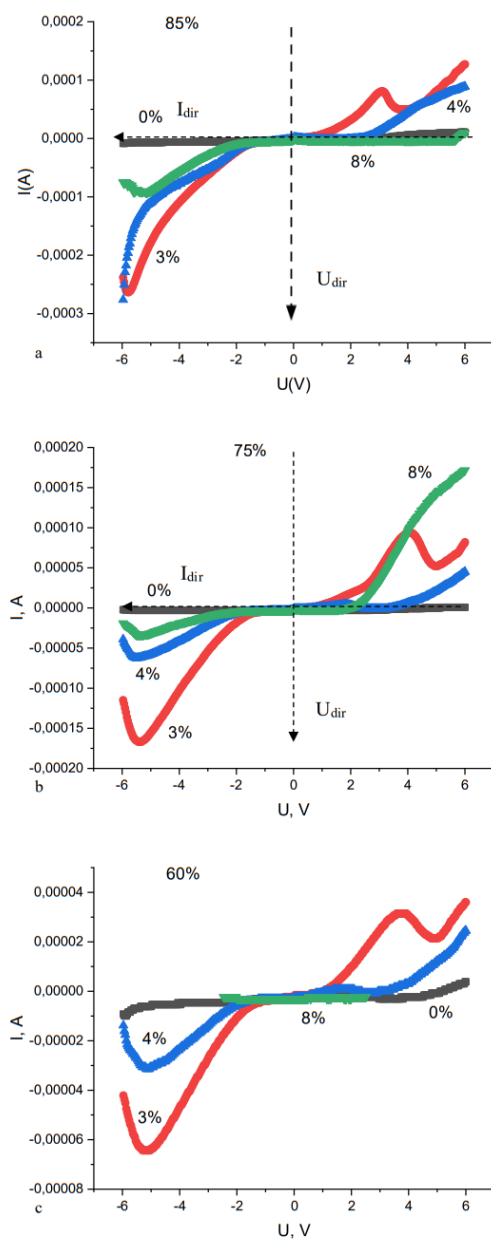


Fig. 6. dependence of current on voltage at contacts 400-600 based on nanopowders with yttrium content  $x = 0, 3, 4, 8\text{mol}\%$  at humidity 85% (a), 75% (b) and 60% (c).

Figure 6 shows the current versus voltage dependences for systems differing in the concentration of the alloying component ( $\text{Y}_2\text{O}_3$ ). At all humidity concentrations, there is a clear dependence of the current amplitude on the impurity concentration. A system without an alloying component undergoes minimal changes in the electric field (less than 5-10% of the same value for systems with 3 and 4 mol%  $\text{Y}_2\text{O}_3$ ). An increase in the impurity concentration over 3 mol% leads to a decrease in the current amplitude with an increase in the voltage modulus at the electrodes. I.e., as in the case of size dispersion (Fig. 5), with variations in the impurity concentration in the composition of the material of contacting nanoparticles, the V-I dependences have an extreme character (Fig.6). It can be seen that the value of the limiting current (the direct branch of the V-I characteristic (Fig.6, third quadrant) reaches the maximum value on all spectra (Fig.6) at a concentration of  $\text{Y}_2\text{O}_3$  3 mol% and then sharply (more than twice) decreases with an increase in the impurity concentration by another 1 mol%. An increase in the impurity concentration by more than two times - up to 8% leads to a proportional decrease (approximately by another two times) in the amplitude of the forward branch current, but an increase in the length of the rectilinear section of the reverse branch. The latter effect depends on the concentration of moisture in the system and is most pronounced when the vapor concentration corresponds to a relative humidity of 80%. It should be noted that under the same conditions, the maximum effect is achieved in terms of the value of the forward current in the case of a system with 3 mol%  $\text{Y}_2\text{O}_3$ . Thus, the concentration of humidity vapor corresponding to 85%, as in the case of the dimensional dispersion (Fig. 5), ensures that the system reaches the maximum limiting parameters corresponding to a particular concentration of impurities. A decrease in the concentration of humidity in the system leads to a decrease in the level of electrical characteristics of the contact, which characterize its rectifying properties. In particular, both the level of limiting characteristics and the nature of the dependences decrease, in particular, the contact passes from the state of a rectifying contact with the most pronounced asymmetry of the V-I curve in the first and third quadrants to the state of the so-called "false connection".

### Conclusion (experiment).

The dependences of the electrical properties of the contact of two objects, consisting of nanoparticles of the same chemical composition, but of different sizes, on the content of the alloying component and the dispersion of the particle size at different moisture content in them are investigated in direct current. A general pattern has been established for the systems under study, which consists in the extreme nature of changes in the limiting electrical properties of contacts, depending on the size dispersion and impurity concentration in the material of contacting nanoparticles. It is assumed that the extreme behavior of the electrical properties of the system is due to the concentration constraint on the number of mobile charge carriers with an increase in the particle size and stabilization of their phase composition.

A general pattern has been established for the systems under study, which consists in the dependence of the nature of the electrical properties on the moisture content in the samples. In particular, it has been found that at low moisture content (saturation in a humid atmosphere at 60% relative humidity), a "False connection" contact occurs. As the relative humidity of the atmosphere in which the system was saturated to 85% (free water in the pores) increases, the nature of the contact changes to semiconductor, which indicates a significant role of the dimension of electrical conductivity (2d or 3d) in the formation of the semiconducting properties of the contact.

## 4. Interpretation of the effect.

### 4.1. The nature of the electronic component in ionic nanocrystals.

According to [27], adsorption significantly changes the electronic structure and physical properties of the material of nanoparticles; in particular, it imposes a spectrum of local levels of adsorbates (surface states of impurity type) on the energy spectrum of states of non-adsorption origin. This, first of all, leads to recharge of the surface and localization in the near-surface region of nanoparticles of charge carriers. The acceptor nature of the adsorption electronic state, the surface is charged negatively, in a thin layer (Debye screening length)  $L = f(\epsilon, T, n)$  near the surface, a p-type space charge region (SCR) is formed [28]. This is shown in an increase in the conductivity of the near-surface layer of nanoparticles and the overall conductivity of the system [29], and in the appearance of a relatively high electrical capacity in the nanopowder system and the possibility of charge exchange with the external environment [30].

The assumption of adsorption-induced localization of electron-type charge carriers (formation of "electron gas") in the near-surface region of nanoparticles is confirmed by molecular dynamics (MD) calculations. In [31] MD methods have shown a sharp increase in the density of localized electronic states in the band gap (BG) during the adsorption of moisture on the surface of the  $\text{ZrO}_2 - \text{Y}_2\text{O}_3$  crystal.

The magnitude of the surface potential depends on the number of molecules adsorbed on the surface and on the size and shape of the particle surface itself. Surface geometry leads to a significant modification of Tamm states. So, we can distinguish: the stretching of Tamm's orbitals outside the particle with a decrease in its size [32] (the formation of chemically uncompensated valence orbitals - "dangling bonds" capable of "capturing" incident molecules from the gas phase); an increase in the Coulson free valence index of Tamm orbitals with an increase in the curvature of the surface [33]; shift of a pair of levels of Tamm states to the middle of the band gap as the curvature of the surface of nanoparticles in ionic crystals increases (decrease in the effective band gap) [34] – a decrease in the electron localization energy when the energy bands are curved as a result of surface charging. For example, adsorbates, there



is a "collapse" of the forbidden zone during the adsorption of water molecules. [12, 35]. According to [36], the magnitude of the field between the volume and the surface of nanoparticles (surface potential) depends on the particle size  $d$  in the range  $-1 \leq d/2L_{eff} \leq -2.2$  due to the overlap of the SCR from opposite surfaces.

#### 4.2. Electronic mechanism.

The proposed mechanism is based on the assumptions about the confinement of electronic excitations and the commensurability of the number of surface and bulk electronic states [37] inherent in nanoscale objects. The zone model of Tamm (1932) modified with the use of fractal geometry makes it possible to consider the form factor of the surface of nanosized objects and can be used to describe the electro-surface effects considered in this work [38, 39].

The classic Madelung-Seitz diagram [40] shows the energy levels as a function of the interatomic distance  $R$  in ionic crystals of type AB (eg NaCl) with one limited surface (Fig. 7). According to Seitz [32], the band gap energy is directly related to the Madelung energy, both in the volume and on the surface.

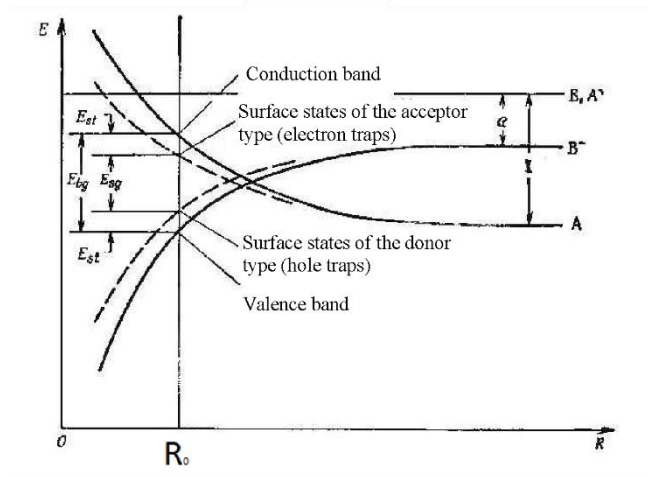


Fig. 7 Classical energy diagram of Madelung-Seitz in ionic crystals of type AB.

Indeed, in fig. 7, which reproduces Seitz's reasoning, shows the origin of the solid-state electronic spectrum from the electronic spectrum of NaCl atoms. Obviously, that the width of the band gap in the crystal volume is a function of the size/shape of the crystal (conditioned by the Madelung constant in the bulk ( $L_b$ ) as well as on the surface ( $L_s$ )). It is clear that  $L_s < L_b$ , since the Madelung sums for a surface ion are approximately half as large as the volume sums. Simple physics makes it possible to understand that, in this case, "two Tamm levels" on the surface have a very simple genesis - these are the levels of the edges of the conduction band and the valence band tightened to the middle of the band gap (Fig. 8, a).

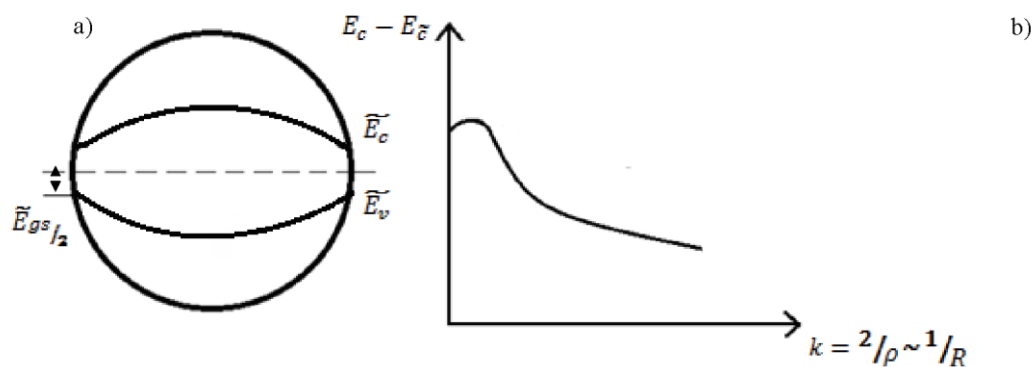


Fig. 8 Schematic representation of the energy level of an impurity of a spherical nanoparticle and the dependence of its energy on the surface curvature  $R$  in the representation of a two-zone model.

Thus, the energy distance between two levels near the surface (donor and acceptor) is less than the band gap in the bulk.

According to [30, 31], for an ion located at the top of a convexity in the case of a convex surface, when calculating the Madelung energy, new additional regions of the crystal with ions located in them will no longer be enough. This immediately leads to a further shift of the "two Tamm levels" towards the middle of the forbidden band in Fig. 8.

The dependence of the band gap on a curved surface on the degree of its curvature has the form  $k = \frac{2}{\rho}$ , where  $\rho$  is the radius of curvature, and with increasing curvature, the surface band gap decreases ( $\frac{d}{dR}E_{gs} > 0$ ), fig.8 b.

In the case of contact of two spherical nanoparticles with  $R_1 > R_2$  with an ionic bond (Fig. 1c), there is a heterojunction of identical materials, but of different particle radii. With a sufficient degree of similarity, we can speak here as about the contact of two graded-gap semiconductors, but in order to reveal the most important property of such a structure - the contact potential difference, it is possible to ignore the variation-gap in the first approximation. It is easy to show that the confinement of electron-hole excitations in nanoparticles of different radii leads to a difference in the ionization potentials and electron affinity energies in these particles with different radii, which immediately destroys the equality of the Fermi level in these two samples even in the absence of alloying. If there is a deep level from a certain defect (alloying impurity) in the band gaps on the surfaces of the contacting particles, provided that it does not coincide with the Fermi levels due to the smallness of these band gaps, the wave function of such an electronic state on the defect is a kind of superposition of the eigenstate of the defect, states conduction and valence bands (Keldysh 1963) [41, 42]:

$$\psi_i(z) = \psi_0(z) + \int_{cz} c(\varepsilon) \varphi_k(\varepsilon) d\varepsilon + \int_{vz} \tilde{c}(\varepsilon) \tilde{\varphi}_k d\varepsilon, \quad (1)$$

where cz - conduction zone; vz - valence zone.

Here, the coefficients  $c(\varepsilon)$  and  $\tilde{c}(\varepsilon)$  give weight factors for the contribution of the respective zones. Assuming that the electronic spectra of the conduction and valence bands are described by the dispersion law:

$$E_{1,2} = \pm \left[ \left( \frac{\widetilde{E}_{gs}}{2} \right)^2 + \left( \frac{\widetilde{E}_{gs}}{2} \right) \rho^2 \div m \right]^{\frac{1}{2}}, \quad (2)$$

and the intrinsic defect field represents the value of the Coulomb potential, the energy of the local state has the form [43, 44]:

$$E_i = \left( \frac{\widetilde{E}_{gs}}{2} \right) \left[ 1 - \frac{2me^4 z^2}{\hbar^2 \xi \widetilde{E}_{gs}} \right] \quad (3)$$

where,  $\xi$  is the permittivity, and the energy is measured from the middle of the band gap. Formula (3) actually corresponds to the two-zone model of the "hydrogen atom" system in the relativistic approximation). The remarkable feature of this result is the non-linear dependence of the depth of the defect level on the band gap (on the surfaces). Therefore, for nanoparticles of different sizes, the depths of the impurity (or defect) levels will necessarily differ, and the stronger, the more the radii of these nanoparticles differ (Fermi levels  $F(R_1) \neq F(R_2)$ ). This difference immediately leads to the presence of a contact potential:

$$U_k \sim f(R_1, R_2) \cdot \Delta R \quad (4)$$

Obviously, the origin of such a contact potential is a new mechanism.

In the framework of the two-band impurity model from the general equation of electrical neutrality, the value of the contact potential difference ( $U_k$ ) for two contacting spherical nanoparticles of different radius ( $R_1 > R_2$ ), provided that the impurity level is a donor level with energy  $E_D$ , has the form:

$$n_0 \cdot \frac{4\pi^2 \hbar^3}{A} = (2\pi m_e k_0 T)^{\frac{3}{2}} \cdot \left( 1 + A \cdot \exp\left(\frac{E_D}{k_0 T}\right) \right), \quad (5)$$

where  $n_D$  - impurity concentration

The solution of the equation for the case of high temperatures has the form:

$$E_F = \frac{n_D \pi^3 \hbar^3}{(2\pi m_e k_0 T)^{\frac{3}{2}}}, \quad (6)$$

The Fermi level ( $E_D$ ) does not depend on the nanoparticle radius and

$$V_{1c} = E_F^{(1)} - E_F^{(2)} = 0, \quad (7)$$

in the case of identical donors, the contact potential difference is zero at high temperatures. In the case of low temperatures, the solution has the form:

$$E_F = -\frac{\varepsilon_D}{2} + \frac{1}{2}k_0T \cdot \frac{\ln((2\pi\hbar)^3 n_D)}{2(2\pi m_e k_0 T)^2}, \quad (8)$$

The contact potential difference is determined by the dependence of the depth of the donor levels on the radius of the nanoparticles:

$$U_k = E_F^{(1)} - E_F^{(2)} = \frac{|\varepsilon_D(R_1) - \varepsilon_D(R_2)|}{2}, \quad (9)$$

## Conclusion

For the first time, a semiconductor structure in the form of a contact of chemically homogeneous nanoparticles has been practically implemented and studied, which is based on the size effects of band structure distortion that occur when scaling physical objects to a low-dimensional range. The results of the project implementation confirm the assumption of the possibility of practical implementation of new semiconductor structures without the use of chemically inhomogeneous materials and the possibility of overcoming the basic problem of modern semiconductor electronics associated with diffusion instability of semiconductor heterostructures. Replacing classical heterojunctions will make it possible to approach the creation of fundamentally new electronic devices and devices that can operate under extremely harsh temperature conditions, have optical transparency, mechanical strength, or biocompatibility, and at the same time have submicroscopic dimensions.

For the studied systems, a general pattern has been established, which consists in the dependence of the nature of the electrical properties on the size of the contacting particles and the moisture concentration in the samples. In particular, it was found that at a low moisture concentration (saturation in a humid atmosphere at a relative humidity of 60% (an island layer of water molecules on the surface of nanoparticles) a “false bond” type contact takes place. At an atmospheric humidity of 85%, the system is saturated (free water in pores) and the change in the nature of the contact conductivity changes to semiconductor, which indicates a significant role of the nature of the distribution of moisture in the pore volume in the formation of the semiconductor properties of the contact. And, a nonlinear properties of contact of objects with the same particle size are leveled as the concentration of moisture molecules increases.

The effect practically does not manifest itself upon contact of monodisperse particles. The difference in particle sizes  $d_i$  ( $i = 400, 500, 600, 700$  – is the designation of a nanostructured object) leads to an almost proportional increase in the reverse voltage ( $d400/d700 = 1,8$ ;  $U700/U400 = 1,9$ ), but a decrease in the current.

The calculated electrical power of the resulting device does not depend significantly on the difference in the sizes of the contacting nanoparticles and, other things being equal, is 4,86 mW for the 400-500 system (4.9mW for the 400-600 and 400-700 systems).

The experiment proves the difference in some electrical and electronic properties of the generalized surface of different-sized particles.

Theoretical ideas about the electronic structure near the surface in the case of ionic crystals undergo certain changes. First, for a flat surface, variance of electronic zones is realized, since the band gap on the surface is less than in the bulk, and second, the convexity of the surface of nanoparticles further enhances the variance of electronic zones.

By applying the Keldysh model (1963) to the problem of the depth of the defect or impurity level, it was shown that in ionic nanoparticles of different sizes, a nonlinear dependence of the depth of the defect level on the radius of the nanoparticle is realized. This leads to the appearance of a contact potential difference.

Of particular note is the question of the nature of peaks on the reverse branch of the VAC. It can be assumed that such an unusual pattern is associated with the existence of an inverted jagged potential hole. Indeed, as the reverse voltage increases (the negative electrode is connected to a small nanoparticle), the lower part of the tooth first intersects with the upper boundary of the band gap of the small nanoparticle, and the peak ends with the E boundary reaching the end of the potential hole of the tooth and the transition of electrons from the small nanoparticle to region of the continuous spectrum. This hypothesis needs further analysis.

**Acknowledgments.** The study was performed in the scope of the H2020/MSCA/RISE/SShare number 871284 project, RO-JINR project No. 366 / 2021 item 81, RO-JINR grant No. 367 / 2021 item 27 and Poland-JINR Projects No. 168 / 2021 item 26.

## References

- 1 Kakurin, Yu. B. Modeling of diffusion processes in inhomogeneous structures of solid-state electronics: specialty 05.27.01 "Solid-state electronics, radio-electronic components, micro- and nanoelectronics, devices based on quantum effects" : dissertation abstract for the degree of candidate of technical sciences / Kakurin Yuri Borisovich . - Taganrog, 2009. - 16 p. – EDN NLCOLD.
- 2 Mladenov G. M. et al. Nanoelectronics. In 2 books. Book. 1. Introduction to nanoelectronic technologies. – 2010.
- 3 Zhang T., Hu C., Yang S. Ion Migration: A “Double-Edged Sword” for Halide-Perovskite-Based Electronic Devices //Small Methods. – 2020. – T. 4. – №. 5. – C. 1900552.
- 4 Dai J. J. et al. High hole concentration and diffusion suppression of heavily Mg-doped p-GaN for application in enhanced-mode GaN HEMT //Nanomaterials. – 2021. – T. 11. – №. 7. – C. 1766.
- 5 Salehzadeh O. et al. Edge Breakdown Suppression of Avalanche Photodiodes Using Zn Diffusion and Selective Area Growth //IEEE Photonics Technology Letters. – 2019. – T. 31. – №. 10. – C. 767-770.
- 6 Qin P. et al. Metal ions diffusion at heterojunction chromium Oxide/CH<sub>3</sub>NH<sub>3</sub>PbI<sub>3</sub> interface on the stability of perovskite solar cells //Surfaces and Interfaces. – 2018. – T. 10. – C. 93-99.
- 7 Ma J. et al. Efficient and stable nonfullerene-graded heterojunction inverted perovskite solar cells with inorganic Ga<sub>2</sub>O<sub>3</sub> tunneling protective nanolayer //Advanced Functional Materials. – 2018. – T. 28. – №. 41. – C. 1804128.
- 8 Nikiforova N. N. et al. FRACTAL NANOCATALYSIS AND RELATED PHENOMENA // Surface. X-ray, synchrotron and neutron studies. – 2018. – no. 2. - S. 68-73.
- 9 Doroshkevich A.S., Shilo A.V., Saprykina A.V., Konstantinova T.E., Danilenko I.A. Impedance spectroscopy of highly concentrated nanopowder disperse systems based on zirconium dioxide // Proceedings of the conference SMMT 2011 November 16-18, 2011. - 2011. P.103.  
Shilo A.V., Doroshkevich A.S., Saprykina A.V., Konstantinova T.E., Danilenko I.A., Tkachenko A.M. The surface of nanopowders based on ZrO<sub>2</sub> as a container for energy conservation // Proceedings of the CMMT 2011 conference November 16-18, 2011. - 2011. P. 216.
- 10 A. Lyubchyk, H. Águas, E. Fortunato , R. Martins, O. Lygina, S. Lyubchyk, N. Mohammadi, E. Lähderanta, A. S. Doroshkevich, T. Konstantinova , I. Danilenko, O. Gorban, A. Shylo, V. K. Ksenevich, N. A. Poklonski Experimental evidence for chemo-electronic conversion of water adsorption on the surface of nanosized yttria-stabilized zirconia // Proceedings of international conference nanomeeting Physics, Chemistry and Application of Nanostructures, 2017, pp. 257-263 DOI:10.1142/9789813224537\_0059.
- 11 A. S. Doroshkevich, A. I. Lyubchyk, A. V. Shilo, T. Yu. Zelenyak, V. A. Glazunovae, V. V. Burhovetskiy, A. V. Saprykina, Kh. T. Holmurodov, I. K. Nosolev, V. S. Doroshkevich, G. K. Volkova, T. E. Konstantinova, V. I. Bodnarchuk, P. P. Gladyshev, V. A. Turchenko, S. A. Sinyakina Chemical-Electric Energy Conversion Effect in Zirconia Nanopowder Systems. Journal of Surface Investigation: X-ray, Synchrotron and Neutron Techniques, 2017, Vol. 11, No. 3, pp. 523–529. DOI: 10.1134/S1027451017030053.
- 12 Doroshkevich A.S., Matuzenko A.A., Saprykina A.V. Danilenko I.A., Konstantinova T.E., Nosolev I.K., Shilo A.V., Akhkozov L.A. The effect of charge accumulation with compacts of old powders based on zirconium dioxide // Proceedings of the conference FTT 2011, Minsk .: A.N. Varksin. Editors: D.A. Zhukovets, S.I. Galai et al., October 18-21, 2011. 2011. V.2. pp.266-268
- 13 Invention Patent RU2729880C1 “Solid-state capacitor-ionistor with a dielectric layer made of dielectric nanopowder” Doroshkevich A. S., Shilo A. V., Zelenyak T. Yu., Konstantinova T. E., Lyubchik A. I., Tatarinova A. A., Gridina E. A., Doroshkevich N. V. <https://patenton.ru/patent/RU2729880C1>
- 14 Poltoratskaya A.V., Shilo A.V., Doroshkevich A.S. DIMENSIONAL ELECTROKINETIC EFFECT OF THE APPEARANCE OF PERIODIC CURRENT PULSATIONS IN COMPACTS FROM ZIRCONIUM DIOXIDE NANOPOWDER AFTER ELECTROSTATIC EXPOSURE // InternationalConference "FunctionalMaterials" Partenit, Crimea,UkraineSeptember 29 - October 5, 2013. P.418.

- 15 A. S. Doroshkevich, I. A. Danilenko, T. E. Konstantinova, G. K. Volkova, V. A. Glazunova Structural Evolution of Zirconia Nanopowders As a Coagulation Process // Crystallography Reports, 2010, Vol. 55, No. 5, pp. 863–865.
- 16 A.S. Doroshkevich, I.A. Danilenko, I.A. Yashchishin., T.E. Konstantinova, V.L. Beardless, G.K. Volkova, V.A. Glazunova, L.D. Perekrestova, V.S. Doroshkevich. Influence of magnetic pulse modification of the surface of ZrO<sub>2</sub> nanoparticles on the processes of their densification. FTVD, 2008, volume 18, No. 3., pp. 133-147.
- 17 Relative humidity of air over saturated solutions / A.G. Tereshchenko - Tomsk, 2010. - 22 p.
- 18 Zirconium dioxide nanopowders and wear-resistant ceramics based on them / I. A. Danilenko, V. A. Fomchenko, T. E. Konstantinova [et al.] // Structures from composite materials. - 2007. - No. 1. - S. 14-21.
- 19 A.S. Doroshkevich, A.I. Logunov, A.V. Shilo, A.I. Lyubchik, A.K. Kirillov, G.A. Troitsky, T.A. Vasilenko, T.Yu. Zelenyak, Yu.Yu. Bacherikov, V.A. Glazunov, V.V. Burkhovetsky, D.A. Suvorov, A.Kh. Islamov, V.S. Doroshkevich, Kh.T. Kholmurodov, E.B. Askerov, A.I. Madazada, MariaBalasoiiu, ValerAlmasan, A.A. Nabiev, T.E. Konstantinova, COMPREHENSIVE STUDY OF A HDD-DENSED NANOSTRUCTURED ZrO<sub>2</sub>-BASED SYSTEM IN THE ASPECT OF SENSOR APPLICATIONS // High Pressure Physics and Technology 2017, vol. 27, no. 3, p.18-31. (<https://elibrary.ru/contents.asp?id=34537559>).
- 20 Artem SHYLO, Oksana GORBAN, Igor DANILENKO, Aleksandr DOROSHKEVICH, Andriy LYUBCHYK, Anton GORBAN, Tetyana KONSTANTINOVA. ELECTROSURFACE PROPERTIES OF NANOPOWDER SYSTEM BASED ON ZIRCONIA // Nanocon - 2019.Oct 16th - 18th 2019, Brno, Czech Republic, EU, Pp. 555 – 560, <https://doi.org/10.37904/nanocon.2019.8565>.
- 21 A.S. Doroshkevich, E.B. Asgerov, A. A. Nabiev, A. Madadzada, Ya. Alieva, A.Kh. Islamov, T.Yu. Zelenyak, A.I. Lyubchik, V.V. Burkhovetsky, V.A. Glazunova, L.V. Loladze, V.S. Doroshkevich, A.V. Shilo, S.A. Sinyakina, A.V. Saprykina, P.P. Gladyshev, Kh.T. Kholmurodov, M. Balashoy, D.M. Khudoba, M.V. Lakusta, T.E. Konstantinova, V.I. Bodnarchuk, Yu.Yu. Bacherikov, R.G. Nazmitdinov Electrical properties of hydrated nanopowder systems based on zirconium dioxide // Proceedings of the scientific seminar in memory of I.L. Khodakovskiy, Dubna, April 6-7, 2017, pp. 70-75. <https://elibrary.ru/contents.asp?titleid=25220> (RSCI).
- 22 ArtemShylo, AleksandrDoroshkevich, AndriyLyubchyk, YuriBacherikov, MariaBalasoiiu, TetyanaKonstantinova. Electrophysicalpropertiesofhydratedporousdispersedsystembasedonzirconiananopowders // AppliedNanoscience <https://doi.org/10.1007/s13204-020-01471-2>.
- 23 A.S. Doroshkevich, A.V. Shylo, V.A. Glazunova, G.K. Volkova, A.K. Kirillov, T. Yu. Zelenyak, V.V. Burkhovetskiy, V.A. Turchenko, V.S. Doroshkevich, A.A. Nabiyeu, T.A. Vasylenko, A. Kh. Islamov, M.L. Craus. Self-organization processes in nanopowder dispersed system based on zirconia under pressure action //Results in Physics. 16 (2020) 102809. doi.org/10.1016/j.rinp.2019.102809.
- 24 Elizaveta A. GRIDINA, Aleksandr S DOROSHKEVICH, Andrey I LYUBCHYK, Artem V SHYLO, Maria Balasoiiu, AkhmedKh. ISLAMOV, Rashid G. NAZMITDINOV Formation and investigation of the properties of composite based on zirconium dioxide ZrO<sub>2</sub> for sensor application ,// 19th International Balkan Workshop on Applied Physics and Materials Science. July 16-19, 2019, Constanta, Romania. P 52.
- 25E.A. Gridina, A.S. Doroshkevich, A.I. Lyubchyk, A.V. Shylo, E.B. Asgerov, A.I. Madadzada, T.Yu. Zelenyak, M.A. Balasoiiu, D. Lazar, V. Almashan, O.L. Orelovich The effect of percolation electrical properties in hydrated nanocomposite systems based on polymer sodium alginate with a filler in the form nanoparticles ZrO<sub>2</sub> - 3mol% Y<sub>2</sub>O<sub>3</sub> // Advanced Physical Research. 2019, Tom 1, №2, (pp.70-80).
- 26 Buzov G.A., Kalinin S.V., Kondratiev A.V. Protection against information leakage through technical channels - M.: Hotline-Telecom, 2005.
- 27 Volkenshtein F.F. Electronic theory of catalysis on semiconductors. M.: IFML, 1960. 216 p.
- 28O. S. Doroshkevych, A. V. Shylo, A. K. Kirillov, A. V. Saprykina, I. A. Danilenko, G. A. Troitskiy, T. E. Konstantinova, T. Yu. Zelenyak Magnetically Induced Electrokinetic Phenomena in the Surface Layers of Zirconia Nanoparticles // Journal of Surface Investigation. X-ray, Synchrotron and Neutron Techniques, 2015, Vol. 9, No. 3, pp. 564–572. DOI: 10.1134/S1027451015030209
- 29 Artem Shylo, Aleksandr Doroshkevich, AndriyLyubchyk, Yuri Bacherikov, Maria Balasoiiu, TetyanaKonstantinova. Electrophysical properties of hydrated porous dispersed system based on zirconia



nanopowders // Applied Nanoscience (Опубликовано онлайн 04.04.2020) <https://doi.org/10.1007/s13204-020-01471-2>.

30 A.S. Doroshkevich, E.B. Askerov, A.I. Lyubchik, A.V. Shylo, T.Yu. Zelenyak, A.I. Logunov, V.A. Glazunova, V.V. Burkhovetskiy, A.H. Islamov, A.A. Nabiev, V.A. Turchenko, V. Almasan, D. Lazar, M. Balasoiu, V.S. Doroshkevich, A.I. Madadzada, A.I. Beskrovny, V.I. Bodnarchuk, Yu.Yu. Bacherikov, B.I. Oksengendler Direct transformation of the energy of adsorption of water molecules in electricity on the surface of zirconia nanoparticles // Applied Nanoscience. 9(8), 1603-1609 DOI 10.1007/s13204-019-00979-6.

31 Mekhrdod Subhoni, Kholmirdzo Kholmurodov, Aleksandr Doroshkevich, Elmar Asgerov, Tomoyuki Yamamoto, Andrei Lyubchik, Valer Almasan, Afag Madadzada Density functional theory calculations of the water interactions with ZrO<sub>2</sub> nanoparticles Y<sub>2</sub>O<sub>3</sub> doped //: Journal of Physics: Conf. Series 994 (2018) 012013. doi :10.1088/1742-6596/994/1/012013

32 Oksengendler B.L., Askarov B., Nikiforov V.N. // JTF. 2014. V. 84. No. 10. S. 156.

33 Oksengendler B.L., Turaeva N.N. // Dokl. RAN. Physics. 2010. V. 434. No. 5. S. 609.

34 Askarov B., Vohidova N., Oksengendler B.L. etc. // Uzbek. chem. journal 2016. Vol. 1. S. 32.

35 Yasuharu Okamoto First -principles molecular dynamics simulation of O<sub>2</sub> reduction on ZrO<sub>2</sub> (111) surface // Applied Surface Science 255 (2008) 3434–3441

36 Yuriy Yu. Bacherikov & Peter M. Lytvyn, Olga B. Okhrimenko & Anton G. Zhuk & Roman V. Kurichka & Aleksandr S. Doroshkevich Surface potential of meso-dimensional ZnS:Mn particles, obtained using SHS method. // JNanopartRes. (2018) 20:316 <https://doi.org/10.1007/s11051-018-4413-1>

37 I. P. Suzdalev, Nanotechnology: Physical Chemistry of Nanoclusters, Nanostructures, and Nanomaterials (KomKniga, Moscow, 2006) [in Russian].

38 Oksengendler, B.L. and Turaeva, N.N., Surface Tamm states at curved surfaces of ionic crystals Dokl. Phys., 2010, vol. 55, no. 10, pp. 477–479. 15. Oksengendler, B.L., Nikiforov, V.N.

39 B. L. Oksengendler, N.N. Turaeva, A. Ashirmetov, N. V. Ivanov ... Nanofractals, Their Properties and Applications. "Horizon in world physics", N-Y, Nova Science Publishers. 298 (2019); p. 1-36.

40 S. Davidson, J. Levin Surface (Tamm) states. "World"; 1973

41 L. V. Keldysh. Deep levels in semiconductors // ZhETF. 1963. 45. 364-375.

42 K. B. Tolpygo. FTT (1969) 11, p. 2846

43 "The use of accelerator technology for the manufacture of nuclear membranes" Flerov G. N., Apel P. Yu., Didyk A. Yu., Kuznetsov V. I., Oganesyan R. Ts. 274-280. 1989.

44 "Polyimide track membranes for ultra- and microfiltration" Vilensky A. I., Oleinikov V. A., Makov N. G., Mchedlivil B. V., Dontsova E. P. // Vysokomolek. Comm., 36, 3, p. 475-485. 1994.